ISSN 2070-0482, Mathematical Models and Computer Simulations, 2017, Vol. 9, No. 1, pp. 108–119. © Pleiades Publishing, Ltd., 2017.
Original Russian Text © S.V. Sindeev, S.V. Frolov, 2016, published in Matematicheskoe Modelirovanie, 2016, Vol. 28, No. 6, pp. 98–114.

Modeling the Hemodynamics of the Cardiovascular System with Cerebral Aneurysm

S. V. Sindeev and S. V. Frolov*

Biomedical Engineering Department, FSBEI HPE Tambov State Technical University, Tambov, Russia

**e-mail: sergej.frolov@gmail.com*

Received December 21, 2015

Abstract—A method of multiscale hemodynamics modeling is presented, which allows coupling the mathematical models of hemodynamics with a different level of detail for the preoperational evaluation of patients' condition with cerebral aneurysm. The simulation results can be used by a physician for developing a strategy and tactics of treatment according to the individual features of the cardiovascular system of a patient.

Keywords: cerebral circulation, cardiovascular system model, genesis of aneurysm, multiscale mathematical model, model of global hemodynamics, hemodynamics model of arterial tree, model of cerebral artery hemodynamics, high performance computing

DOI: 10.1134/S2070048217010148

INTRODUCTION

The causes of the occurrence and development of cerebral aneurysm are still obscure. It is suggested that changes in local and global hemodynamics play a key role in the formation and subsequent development of aneurysms [1]. Investigation of hemodynamics is a major task in the study of the genesis of aneurysms and during the evaluation of the preoperative condition of the patients. It is done based on physical and mathematical simulations.

Experimental setups for the simulation of a single vessel have come to be broadly used for studying the genesis of the cerebral aneurysms and their treatment. For example, an interrelation between high wall shear stress and the probability of the formation of aneurysm in cerebral arteries was revealed based on the experimental simulation studies [2]. The effect of the stenting treatment method on the local hemodynamics of a cerebral vessel in order to prevent restenosis was also studied in simulation experiments [3].

A computational investigation of hemodynamics is the most developed method today. The following mathematical models of the cardiovascular system (CVS) are known: global hemodynamics models (0D models), models of hemodynamics of arterial tree (1D models), and three-dimensional vessel hemodynamics models (3D models). CVS is represented in 0D models by separate elements connected with each other [4, 5]. An elastic chamber filled with blood is used as an element. Each connection between the chambers is characterized by the speed of the blood flow, which does not depend on a spatial coordinate. This kind of models describe the behavior of the blood flow sufficiently precise however, it is not suitable for studying cerebral hemodynamics due to the fairly rough assumptions about the locality of the hemodynamic parameters.

It is assumed in the models of the arterial tree that the hemodynamic functions, such as blood flow and blood pressure, alter along the length of a vessel (so that there is only one dimensional coordinate, 1D) [6, 7]. In addition, the dependency of vessel's cross-section area on the pressure is considered, and the pressure is set quasi-linear in most studies. An advantage of 1D models is their ability to study the propagation of a pulse wave along the arterial system. However, these models have found only limited use in studying cerebral hemodynamics and methods for treatment of cerebral circulation disorders, since these models do not reflect the velocity distribution in the cross-section of a vessel, which is important in analyzing the risk of the formation of aneurysm.

Three dimensional models (3D models) of vessel hemodynamics are the most precise today. These models are developed based on the Navier-Stokes equation, and they describe three-dimensional blood flow only in a separate part of the CVS, more often in a single artery or a bifurcation. Such an approach

is characterized by a long computation time of a system of equations for the model. Although, as the analysis of the literature has shown, 3D models are used in particular as a major tool for the analysis of the genesis and treatment methods of cerebral aneurysms.

Among Russian studies devoted to the mathematical simulation of hemodynamics, including the simulation of cerebral blood circulation, the studies conducted at the Faculty of Computational Mathematics and Cybernetics of Lomonosov Moscow State University are worth noting. Quasi one-dimentional approximation is used in several works [8–11], where the whole CVS is represented by a graph consisting of bonds and state points, which is to say, there is a model of the hemodynamics of the arterial tree (1D model). The mathematical models of hemodynamics taking into account the features of cerebral blood circulation and the vascular structure of the brain are presented in another study [8]. A number of effective numerical algorithms for the solution of equations in cerebral hemodynamics on the vascular graph are developed in [9]. For the first time, a number of sophisticated CVS models are suggested, which include the simulation of blood circulation in separate organs such as the kidney and gastrointestinal tract [11]. A set of heart models in lumped parameters built on the experimental dependences of the flow and pressure in the left ventricle is presented in [11]. The numerical studies of blood circulation in the brain are performed in healthy conditions and pathologies. However, blood flow is considered to be one-dimensional in the simulation of cerebral circulation, and this does not allow us to fully reveal the factors affecting the genesis and treatment of cerebral aneurysms; the influence of global hemodynamics factors on cerebral circulation is not taken into account; the action of the heart is simulated by an experimental dependency, and this does not give an opportunity to study the influence of heart pathologies on cerebral circulation.

Among Russian studies focused on the simulation of cerebral circulation, it is necessary to distinguish those studies performed at Chernyshevskii Saratov State University [12–17]. The authors' main scientific interest lies in the investigation of the influence of the mechanical properties of the vascular walls in Willis's circle on the formation of aneurysms in cerebral vessels. The authors performed a series of natural experiments on the lateral and transversal stretching of the vessels of Willis's circle [12, 13]. As a result, the values of the deformational-strength characteristics were obtained. The role of congenital defects in the cerebral arteries' walls in the genesis of aneurysms is reported in the studies. The obtained characteristics are used further for studying brain arteries in normal conditions and in the presence of aneurysm by the mathematical simulation methods [14]. The 3D hemodynamics models developed by the authors are used for the simulation of hemodynamics in the arteries of Willis's circle. Analyzing the results of the mathematical model computation for the hemodynamics of the arteries of Willis's circle, the authors identify key factors leading to the genesis of vascular pathologies: they are shear stress and blood pressure [15]. The numerical study of hemodynamics in the carotid artery with a normal structure and pathological curvature was performed [16]. Blood is represented by the incompressible Newtonian fluid in this study. As a result of the numerical experiments with the carotid artery models with different structural pathologies, the profound influence of the curvature of the carotid artery was revealed on the hemodynamic parameters of the blood flow, which leads to atherosclerosis. The simulations showed that the low values of the wall shear stress lead to both the formation of atherosclerotic plaques and the rupture of aneurysms. It was revealed that blood pressure near the bifurcation apex has maximum values during the whole cardiac cycle, which could be a reason of the wall weakening and the formation of aneurysm in the apex region. The results of the studies showed that the wall deformations of a weakened region are substantially larger than the wall deformations of a healthy artery. These deformations allow to demonstrate the initial stage of the formation of aneurysm. In [17] a problem for simulating blood flow in a system of vessels with elastic walls was formulated and a method for constructing realistic geometrical models of the vessels of Willis's circle in the brain based on the results of magnetic resonance tomography was presented. However, cerebral hemodynamics is considered separately from the factors of global hemodynamics in [12–17]; the results of the numerical simulation of three dimensional blood flow need to be compared with the experimentally obtained data; the blood is represented as an incompressible Newtonian fluid.

There are several foreign studies aimed at investigating the treatment methods and the genesis of cerebral aneurysms, which should be mentioned. A series of experiments on determining the mechanical properties of the walls of cerebral aneurysms is described in [18]. The results have shown a substantial difference in the mechanical properties between healthy arteries and aneurysm. The authors hypothesized that the rupture of separate collagen fibers composing the wall of the aneurysm leads to the rupture of the whole aneurysm [19]. The numerical experiments revealed several parameters resulting in the rupture of aneurysm. A mechanistic-biological model of the arterial tissue was used to evaluate the long-standing efficiency of the stenting procedure [20]. The results of the computation of three dimensional blood flow along an idealized artery revealed that different modifications of the stents result in the formation of neointima in different volumes. These volumes could serve as a criterion for the choice of the required

stent modification. It was noted in [21] that the numerical methods of studying the blood flow help better understand cerebral aneurysms hemodynamics and improve the diagnostics and treatment methods.

The analysis of the comprehensive state of the field from 2010 until 2015 revealed the following tendencies. After the development of high performance computation an opportunity appeared to study the genesis and treatment methods of cerebral aneurysms by the numerical simulation experiments with sufficient precision in an acceptable time period. The performed analysis showed that the numerical studies have become prevalent in the investigation of cerebral hemodynamics. However, natural experiments are widely used for studying the biomechanical properties of the walls of the cerebral arteries and aneurysms. Natural experiments are also indispensable for identifying new mathematical models of hemodynamics. A distinct tendency for individualization has appeared in the past five years. The personal morphological features [22–28] and biomechanical properties [29–31] of the cerebral arteries of a specific patient are taken into account.

Although great success is now being achieved in studying reasons for the genesis and treatment methods of cerebral aneurysms, some fields remain obscure. The correlation among disorders in hemodynamics, heart pathologies, and aneurysms genesis has not been considered. Studying the treatment methods of cerebral aneurysms does not take into account the global hemodynamics factors and the state of CVS in general. Blood is represented as the Newtonian fluid in many studies; however, it is known that blood has non-Newtonian properties. The studies do not take into account the dependency of blood viscosity on its flow rate. This confuses the results in some cases of the numerical studies of cerebral hemodynamics. Some studies consider cerebral arteries as vessels with a rigid wall, and this does not allow investigating a vessel deformation depending on the blood pressure. The investigation of the vibrational activity of the wall of the vessel is also not possible in this case.

A new trend in hemodynamics research is the method of multi-scale simulation [32], which is a combined use of the models with a different level of detail coupled by the corresponding boundary conditions. It is worth distinguishing a study among the other works of Russian investigators devoted to a multi-scale simulation of the cardiovascular system [6], where approaches related to the applications of multi-scale hemodynamics models are considered and a method of coupling the one-dimensional model of a single vessel to the zero-dimensional model of a blood vessel is suggested. However, the authors do not consider a method of developing a multi-scale model of the 0D-1D-3D type for studying a chosen cerebral vessel; the used 0D model of global hemodynamics does not fully represent hemodynamic processes in CVS; blood backflow through valves is not taken into account; and the linear and nonlinear models of cardiac output that have been used do not consider the physiological peculiarities of the heart, and this does not allow for the investigation of hemodynamics in the chosen blood vessel in different cardiac pathologies.

This study suggests a conceptual foundation of the multiscale mathematical 0D-1D-3D model of CVS, which allows coupling hemodynamics models of different level of detail for estimating the preoperational state of patients with cerebral aneurysm. The multiscale model could be used for uncovering the dependency of the formation of aneurysm on separate factors of global hemodynamics and cardiac pathologies, and it could also be used for revealing the influence of a cerebral vessel and the factors of global hemodynamics on the risk of the genesis and development of aneurysm, as well as elaborating the recommendations on the treatment of cerebral aneurysms with respect to the individual CVS features of a patient.

An informal formulation of the problem is to define the three-dimensional distribution of blood, its pressure, and wall shear stress in the region of the cerebral aneurysm, given the known shape of the cerebral artery, rheological blood properties of the patient, and global hemodynamics parameters.

MATERIALS AND METHODS

The development of a multiscale model of hemodynamics requires a description of the CVS by a series of models with different level of detail coupled by the appropriate boundary conditions.

2.1 A Model of Global Hemodynamics

The CVS is represented in the model of global hemodynamics as a system of elastic chambers connected by resistance elements and blood flows [4, 5]. The heart is considered as two atria and two ventricles performing a contractile function (active chambers). The cardiac valves are represented by the elements with variable conductivity, which depends on the direction of the blood flow. A generalized structure of the model of global hemodynamics (0D model) is presented in Fig. 1.

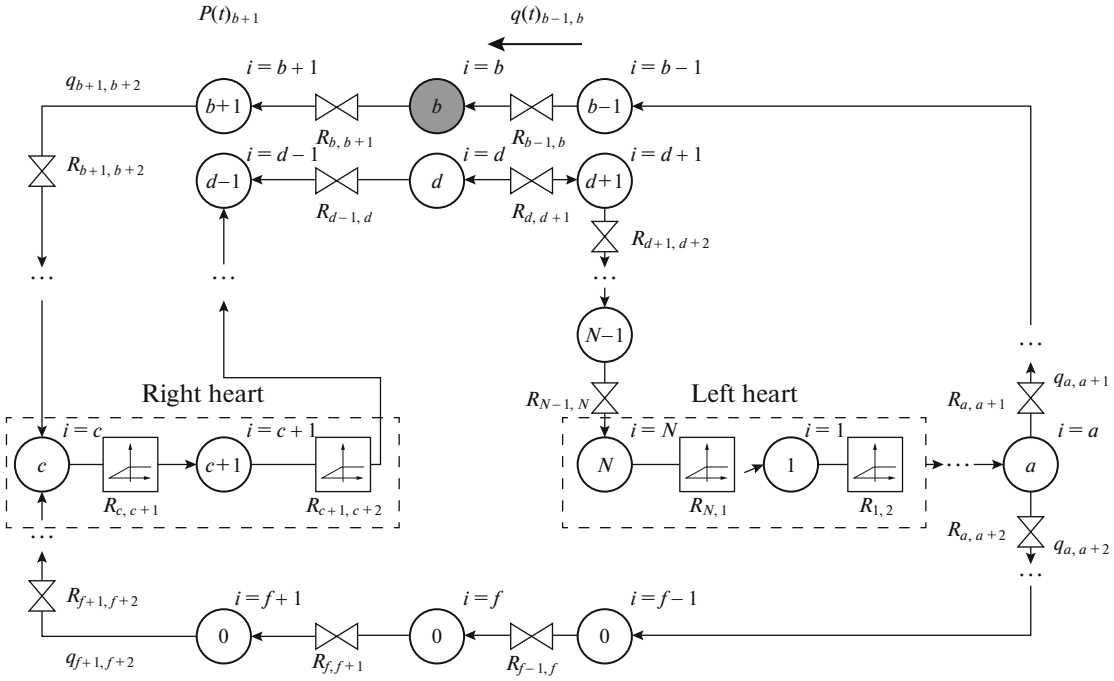

Fig. 1. 0D hemodynamics model structure.

The volume of blood in the chambers of the 0D model is determined by the input and output blood flows

$$\frac{V_i(t)}{dt} = \sum_{i=1}^{N}\sum_{j=1}^{N} w_{ij} \cdot q_{ij}, \quad i = \overline{1,N}, \quad j = \overline{1,N}, \quad V_i(0) = V_i^0, \tag{1}$$

where V_i is the volume of blood in the ith CVS chamber, cm^3; q_{ij} is a blood flow from the ith chamber to the jth chamber, cm^3/s; w_{ij} is a coefficient that determines a connection between CVS chambers; and N is the number of chambers in the 0D model of hemodynamics. The coefficients matrix **W**, which determines the connection between the cameras, could be represented by the elements w_{ij} as

$$\mathbf{W} = \{w_{ij}\} = \begin{cases} 1, \text{ if the flow from the } i\text{th element is included in the } j\text{th element;} \\ -1, \text{ if the flow from the } j\text{th element is included in the } i\text{th element;} \\ 0, \text{ if else.} \end{cases} \tag{2}$$
$$i = \overline{1,N}, \quad j = \overline{1,N}.$$

The equations for the blood flow are written as

$$L_{ij}\frac{d_{ij}(t)}{dt} + R_{ij}(t)q_{ij}(t) = P_i(t) - P_j(t), \quad i = \overline{1,N}, \quad j = \overline{1,N}, \quad i \neq j; \tag{3}$$
$$q_{ij}(t) = q_{ij}^0, \quad R_{ij}(t) = 1/\rho_{ij}(t),$$

where L_{ij} is the blood inertia from the ith chamber into th jth chamber, (torr s^2)/cm^3; R_{ij} is the resistance of the connection (torr s^2)/cm^3; P_i is the pressure in the ith chamber, torr; and ρ_{ij} is conductivity, cm^3/(torr s). Pressure P_i and volume V_i in the passive chamber are interrelated by the equation

$$P_i(t) = \frac{1}{C_i}[V_i(t) - U_i], \quad i = \overline{1,N}; \quad i \neq \{1, c+1\}, \tag{4}$$

where C_i is the elasticity of the ith chamber, cm^3/torr; and U_i is the unstrained volume of the ith chamber, cm^3.

The link between pressure P_i and volume V_i in the cavity of left $i = 1$ and right $i = c + 1$ ventricles is determined by the nonlinear function φ [4, 5, 33]:

$$P_i(t) = \varphi\left(V_i(t), \omega_i(t), \mathbf{A}_i\right), \quad i = \{1, c+1\}, \tag{5}$$

where ω_i is the volume of a pseudo cavity of the ith ventricle, cm^3; and $\mathbf{A}_i$ is the vector of parameters for the ith ventricle.

The vector of the parameters for the ith ventricle $\mathbf{A}_i$ includes

$$\mathbf{A}_i = \left\{h_i, V_i^0, \eta_i, V_i^{es}, V_i^{ed}, k_i, s_i, E_i^{SE}, E_i^{PE}, K_i^{SE}, K_i^{PE}, T_{\text{sys}}(n), T(n)\right\}, \tag{6}$$

where h_i is a thickness of the ventricle wall, cm; V_i^0 is the relaxed ventricle volume, cm^3; η_i is the viscosity coefficient of the myocardium, torr s; V_i^{es}, and V_i^{ed} are the stroke and finite volumes of the ventricle, cm^3; k_i is the pumping coefficient of the ventricle; s_i is the ratio of the contractile fibers in the area of the cross section of the cardiac muscle ($0 < s < 1$); E_i^{SE}, E_i^{PE}, K_i^{SE}, and K_i^{PE} are approximation parameters for tension inside the wall of the chamber; $T_{\text{sys}}(n)$ is the systole duration in the nth cardiac cycle, s; $T(n)$ is the beginning time of the nth cardiac cycle (the beginning of the systole), s; and n is the number of the cardiac cycle.

Relying on myocardium models [4, 5, 33], a special function $\omega_i(t)$ is introduced, which describes the process of ventricle contraction at the systole phase and relaxation at the diastole phase, respectively:

$$\begin{gathered} d\omega_i(t)/dt = Y_1\left(\omega_i(t), \chi_i, u_i\right) \text{ at } t \in [T(n);\ T(n) + T_{\text{sys}}(n)), \\ d\omega_i(t)/dt = Y_2(\omega_i(t), \eta_i, E_i^{SE}, V_i^{SE0}, K_i^{SE}) \text{ at } t \in [T(n) + T_{\text{sys}}(n);\ T(n+1)), \\ \omega_i(0) = \omega_i^0, \quad T(n) = \sum_{\theta=1}^{n} T(\theta), \end{gathered} \tag{7}$$

where V_i^{SE0} is the ventricle's volume consisting of the elements with a constant length, cm^3; and χ_i and u_i are Starling law constants [4, 33].

The resistance of the cardiac valves can be described by the following dependency [4, 33]:

$$R_{ij}(t) = \Omega(\rho_{ij}^*,\ \Delta_{ij}(t),\ \Delta_{ij}^*,\ \beta_{ij}), \quad i, j \in \{(1,2);(c,c+1),(c+1,c+2),(N,1)\}, \tag{8}$$

where ρ_{ij}^* is the conductivity of the open valve, cm^3/(torr s); $\Delta_{ij}(t)$ is the volume of blood moved through the valve in the back direction, cm^3; Δ_{ij}^* is the closing volume, cm^3; and β_{ij} is the coefficient characterizing the rate of decrease of the conductivity of the valve during the blood backflow.

Thus, Eqs. (1)–(8) describe the 0D model of CVS hemodynamics.

2.2. A Model of Hemodynamics of Arteries in the Upper Part of the Body

The next stage is a transition to the one-dimensional model of hemodynamics in the upper parts of the body (the 1D model), which includes the cerebral artery being investigated. This cerebral artery is in chamber b (Fig. 1), which is considered as an assembly of one-dimensional arteries consisting of elastic elementary regions (Fig. 2):

$$b = \bigcup_{k=1}^{K} b_k, \quad b_k = \bigcup_{j=1}^{M_k} b_k^j,$$

where b_k is the kth artery of the upper parts of the body; b_k^j is the jth region of the kth artery; K is the number of arteries in the one-dimensional model of hemodynamics in the upper parts of the body; and M_k is the number of elementary regions in the kth artery.

The dependences obtained based on the model for the elementarily generalized region of a vessel correspond to the elementary region b_k^j [34].

The blood volume in the jth elementary region of the kth artery is related to the flow as

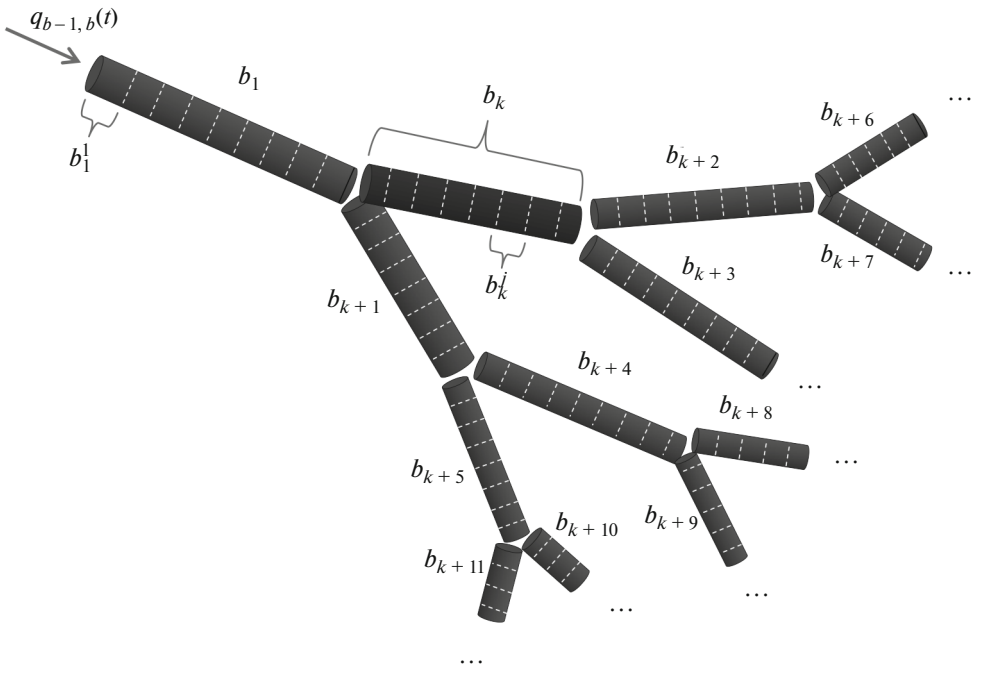

Fig. 2. The region of the arterial bed in the upper part of the body.

$$dV_k^j(t)\big/dt = q_k^{j-1}(t) - q_k^j(t), \quad k = [1;K], \quad j = [1;M_k], \quad V_k^j(0) = V_{0k}^j, \tag{9}$$

where q_k^{j-1} is the blood flow entering the jth region of the kth artery; and q_k^j is the blood flow escaping the jth region of the kth artery.

Equation (9) can be written for a bifurcation:

$$dV_k^j(t)\big/dt = q_k^{j-1}(t) - q_k^{j,k+1}(t) - q_k^{j,k+2}(t), \quad k = [1;K], \quad j = [M_k - 1;M_k], \quad V_k^j(0) = V_{0k}^j, \tag{10}$$

where $q_k^{j,k+1}$ is the blood flow from the jth region of artery k to artery $k+1$; and $q_k^{j,k+2}$ is the blood flow from the jth region of the artery to artery $k+2$.

The blood flow q_k^j in the jth region of the kth artery is proportional to the difference of the pressures in the regions j and $j+1$:

$$q_k^j = \left(P_k^j - P_k^{j+1}\right)\Big/R_j^k, \quad k = [1;K], \quad j = [1;M_k]. \tag{11}$$

Here the resistance R_j^k of the jth region of the kth artery is determined according to Poiseuille's law:

$$R_j^k = \frac{\pi \cdot \left(\left(d_k^{j,\text{prox}} + d_k^{j,\text{dist}}\right)\big/2\right)^4}{128\eta l_k}, \quad k = [1;K], \quad j = [1;M_k],$$

where R_j^k is the resistance of the jth region of the kth artery, cm^3/(torr s); l_k^j is the length of the jth region of the kth artery, cm; η is the dynamic viscosity coefficient of blood, torr s; $d_k^{j,\text{prox}}$ is the proximal diameter, cm; $d_k^{j,\text{dist}}$ is the distal diameter, cm; and P_k^j is the pressure in the jth elementary region of the kth artery, torr.

The pressure in the jth elementary region of the kth artery can be expressed as

$$\begin{aligned} P_k^j(t) &= e_k^j(V_k^j - U_k^j), \quad k = [1;K], \quad j = [1;M_k], \\ U_k^j &= \frac{1}{12}\pi L_k^j\left(d_k^{j,\text{prox}} + d_k^{j,\text{prox}} d_k^{j,\text{dist}} + d_k^{j,\text{dist}}\right), \end{aligned} \tag{12}$$

where U_k^j is the relaxed volume of the jth elementary region of the kth artery.

For adequate use of the one-dimensional hemodynamics model of the upper parts of the body, it is necessary to set the corresponding boundary conditions at the input and the output of the arterial system of the upper parts of the body. The values obtained from the global hemodynamics model (0D model) may be used as these boundary conditions. Accordingly,

$$\begin{aligned} q_1^1(t) &= q_{b-1,b}(t), \\ P_k^{M_k}(t) &= P_{b+1}(t), \end{aligned} \quad k \in [K-W, K], \tag{13}$$

where q_1^1 is the blood flow of the first elementary region of the input artery of the upper parts of the body, cm^3/s; $q_{b-1,b}$ is the blood flow from the aorta into the arteries of the upper parts of the body, cm^3/s; $P_k^{M_k}$ is the pressure in the last elementary region of the output artery of the upper parts of the body, torr; P_{b+1} is the pressure in chamber $b+1$ in the 0D model of hemodynamics, torr; and W is the number of the terminal arteries in the arterial tree model.

The equations mentioned (9)–(13) describe the 1D model of the hemodynamics of the upper parts of the body coupled with the model of global hemodynamics.

2.3. Model of the Local Hemodynamics of the Cerebral Artery

In order to make a transition to the 3D model of hemodynamics in the cerebral artery, the artery of interest b_Z ($k = Z$) (for example, the basilar artery can be chosen) is selected from the assembly of the arteries of the one-dimensional upper parts of the body $b = \bigcup_{k=1}^{K} b_k$. A three-dimensional representation of the selected artery is considered, in which the hemodynamic characteristics of the blood flow speed $u(x, y, z)$ and pressure $P(x, y, z)$ alter in three space coordinates.

Vector $\mathbf{F}$ of the parameters of the cerebral artery b_z can be represented as

$$\mathbf{F} = \left\{\eta\left(du(x,y,z,t)/dn\right),\ \lambda,\ D_{3D}(x,y,z,t)\right\}, \tag{14}$$

where $du(x,y,z,t)/dn$ is the shear rate, s^{-1}; $\eta\left(du(x,y,z,t)/dn\right)$ is the dynamic viscosity of blood at the point (x, y, z) at the time point t, torr s; λ is the density of blood, kg/cm^3; and $D_{3D}(x,y,z,t)$ is the computational domain at the time point t.

The dependency $\eta\left(du/dn\right)$ can be expressed in the case of Newtonian fluid simulation as

$$\eta\left(du/dn\right) = \text{const} = \eta$$

and in the case of non-Newtonian fluid simulation as

$$\eta\left(du/dn\right) = \gamma_{nn}\left(du/dn\right),$$

where γ_{nn} is the nonlinear dependency of blood viscosity on the shear rate.

The movement of blood in the region $D_{3D}(x,y,z,t)$ can be described by Navier-Stokes equations:

$$\frac{\partial \mathbf{u}}{\partial t} + \mathbf{u}\cdot\nabla\mathbf{u} - \eta\Delta\mathbf{u} + \frac{1}{\lambda}\nabla P = 0, \quad \text{div}\,\mathbf{u} = 0. \tag{15}$$

We need to set the corresponding initial conditions for the correct computation of the hemodynamics model in the cerebral artery:

$$u(x,y,z,0) = u_0(x,y,z), \quad P(x,y,z,0) = P_0(x,y,z). \tag{16}$$

The boundary conditions also have to be set:

$$u\big|_{\text{in}}(x,y,z,t) = f_{bc,\text{in}}\left(q_{Z-1}^{M_{Z-1}}(t), S_{Z,\text{prox}}\right), \quad P\big|_{\text{out}}(x,y,z,t) = f_{bc,\text{out}}\left(P_{Z+1}^1(t), S_{Z,\text{dist}}\right). \tag{17}$$

where $u_0(x,y,z)$ is the velocity of blood in the cerebral artery at the initial time moment, cm/s; $P_0(x,y,z)$ is the blood pressure in the cerebral artery at the initial time moment, torr; $u\big|_{\text{in}}(x,y,z,t)$ is the value of the blood velocity at the input boundary of the cerebral artery, cm/s; $q_{Z-1}^{M_{Z-1}}$ is the volumetric blood flow in the first segment of the cerebral artery Z, cm^3/s; $f_{bc,\text{in}}$ is the coupling function of the volumetric flow value at

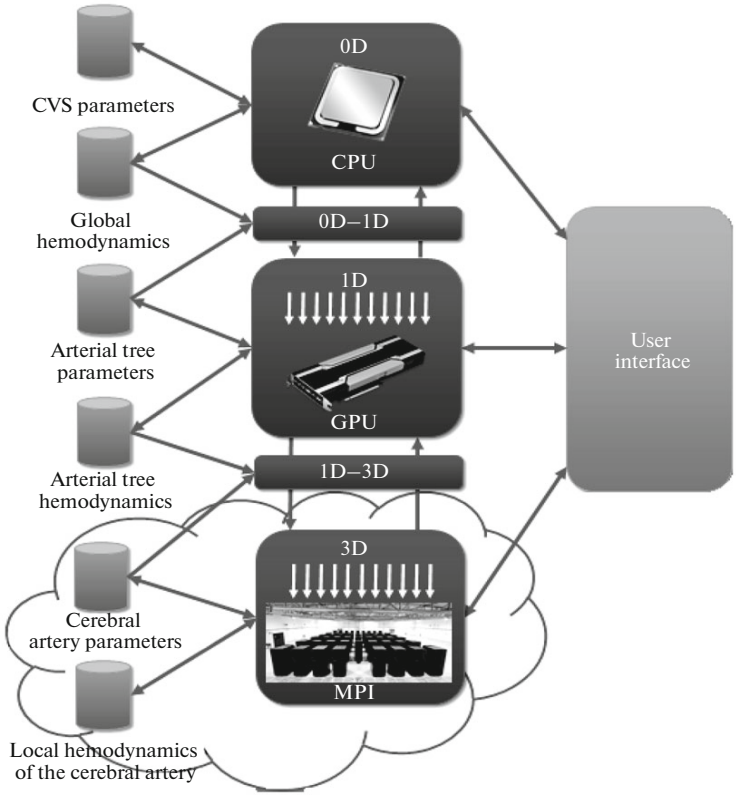

Fig. 3. A scheme of the data exchange among modules of the software complex for the evaluation of the state of preoperational hemodynamics in patients with cerebral aneurysm.

the entrance of the cerebral artery into a three-dimensional profile, which takes into account the position of the artery; $S_{Z,\text{prox}}$ is the area of the proximal part of the cerebral artery, cm^2; $S_{Z,\text{dist}}$ is the area of the distal part of the cerebral artery, cm^2; $P\big|_{\text{out}}(x,y,z,t)$ is the value of the pressure at the output boundary of the cerebral artery, torr; $f_{bc,\text{out}}$ is the coupling function of the output pressure value from the hemodynamics model of the arteries of the upper parts of the body; and P^1_{Z+1} is the value of the output pressure in the cerebral artery obtained from the 1D model of hemodynamics, torr.

Function $f_{bc,\text{in}}$ can be expressed for a laminar blood flow as

$$u\big|_{\text{in}}(x,y,z,t) = u_{\max}(t)\left(1 - \pi r(y,z)^2 \big/ S_{z,\text{prox}}\right),$$
$$u_{\max}(t) = 2q^{M_{Z-1}}_{Z-1}(t)\big/S_{z,\text{prox}}, \quad r(y,z) = (y-y_0)^2 + (z-z_0)^2,$$

where y_0 and z_0 are the coordinates for the center of the cross section of the cerebral artery's proximal region with the area $S_{Z,\text{prox}}$; and $u_{\max}$ is the maximum blood flow speed.

Thus, Eqs. (1)–(17) represent a multiscale model of CVS hemodynamics consisting of the global hemodynamics model (0D model), the model of hemodynamics in the upper parts of the body (1D model), and the model of the local hemodynamics of the cerebral artery (3D model).

3. RESULTS

The method suggested in (1)–(17) was implemented as a set of programs for estimating the preoperational state of patients with cerebral aneurysm. The interaction scheme between the modules of the set is presented in Fig. 3. The modules are identified before running the computation in order to determine the parameters' values for an individual patient. The 0D model is computed at each time step in serial, since this kind of a model has a low computational complexity. At this stage, in addition to the calculation of

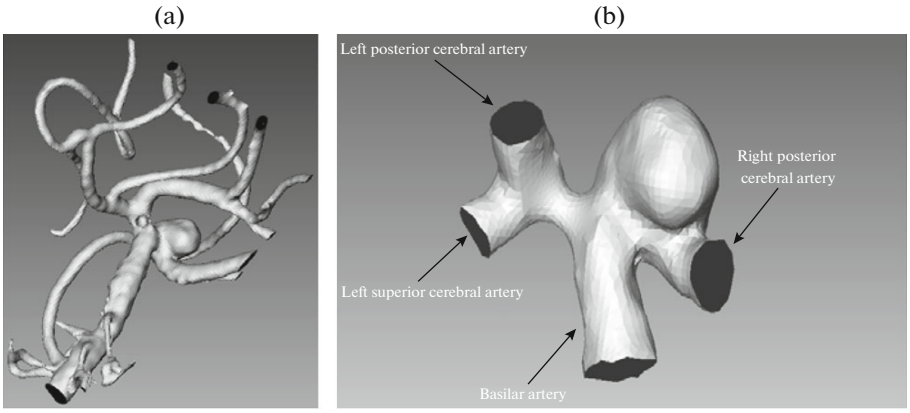

Fig. 4. Segmented CT-angiography data of a patient with basilar artery aneurysm. (a) The region of cerebral arteries. (b) The selected region with aneurysm of the basilar artery.

dependences (1)–(8), the boundary conditions are also determined based on dependency (13) for the 1D hemodynamics model. After the calculation of the 0D model and the boundary conditions for the 1D model, the one-dimensional hemodynamics model (9)–(12) is calculated. Since the computation of the one-dimensional model of hemodynamics is requires complex calculation, the method of parallel computation of this model utilizing GPGPU in the NDIVIA CUDA implementation was suggested. The boundary conditions for the 3D model of hemodynamics are also determined at this stage by using dependency (17). The 3D model of hemodynamics in the cerebral artery has the highest computation complexity. The Lomonosov cluster, which is located at Moscow State University, was used for the computation of this model with the use of MPI technology. After the computation of three-dimensional model of hemodynamics, transition to the next time step of the simulation takes place, and the calculation process is repeated.

A patient with a terminal aneurysm of the basilar artery was chosen as an example. The developed hemodynamics model was identified. The segmented data of the region of the cerebral arteries obtained by CT-angiography and the area of the basilar artery chosen for the calculation are presented in Fig. 4.

According to dependences (1)–(17), the hemodynamics in an individual model of a basilar artery aneurysm were calculated using high-performance computations. The blood flow streamlines at the moment of the systolic peak $T_{sys} = 0.2$ s are presented in Fig. 5. The blood flow has the maximum velocity of 1.14 m/s in the input segment of the bifurcation of the left cerebral artery. This velocity is twice the average speed over the cross section in the input segment of the basilar artery. A nonstable vortex is observed in the aneurysm sac. This may be the reason for the formation of clots inside the aneurysm and the subsequent blockage of the blood flow into the cerebral arteries. The minimum velocity of the blood is observed in the aneurysm sac, where the velocity decreases to 8.94×10^{-7} m/s , and it does not exceed 0.5 m/s, which is about 65% of the axial blood flow velocity, in the inlet segment of the basilar artery.

A crossing plane was chosen for the detailed analysis of the hemodynamics inside the aneurysm. Its position is presented in Fig. 6a. The analysis of the velocity distribution (Fig. 6b) showed that there is a region in the central part of the crossing plane with a low value of the velocity modulus, which alters in the range of $[1 \times 10^{-4}; 0.15]$ m/s. This fact is associated with the existence of a vortex in the central part of the aneurysm due to which a substantial blood volume moves in the direction opposite to the natural flow. At the same time, the area of the maximum blood flow velocities shifts to the dome of aneurysm. The blood velocity in this area alters within a range of [0.25; 0.482] m/s. The average velocity modulus in the crossing section at the moment of the systolic peak is 0.19 m/s, which is only 47% of the average inlet velocity by the cross-section in the initial segment of the basilar artery.

The distribution of the wall shear stress presented in Fig. 7 demonstrates that most of the aneurysm's dome surface is affected by the wall shear stress in the range of [0.2; 2] Pa, which is the critical value underlying the subsequent change in the inner wall layer of the aneurysm cavity and destruction of the endothelium cells. In addition, a significant risk of the further development of the disease is exerted by the bifurcation of the initial segment of the left cerebral artery in the area, where the wall shear stress reaches its maximum value of 40 Pa, which also may lead to a disruption of the inner wall layer of the cerebral artery.

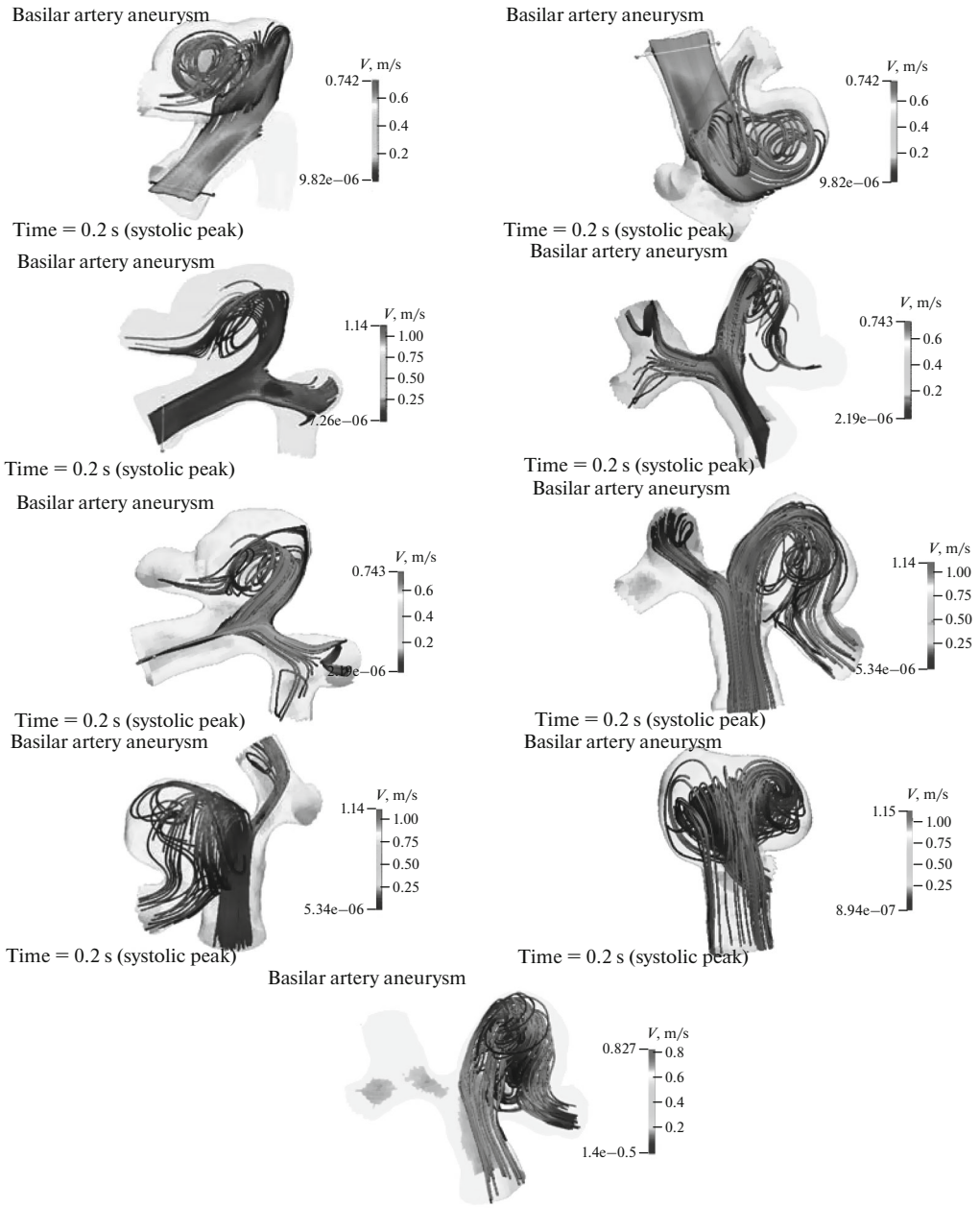

Fig. 5. Streamlines for an individualized model of aneurysm of the basilar artery.

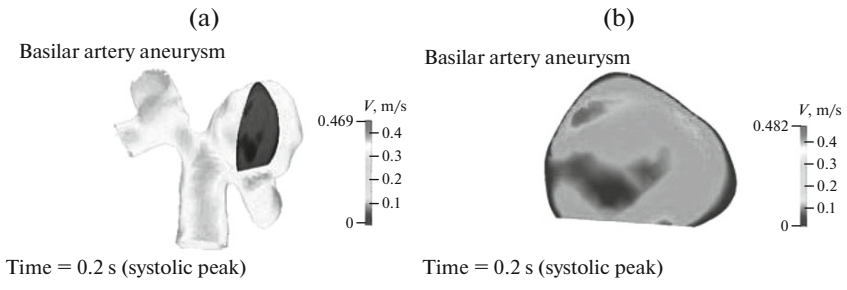

Fig. 6. A cross section of the aneurysm model. (a) Location of the crossing plane. (b) The crossing plane.

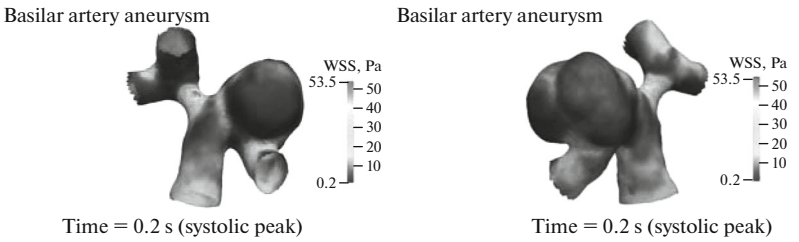

Fig. 7. Wall shear stress at the moment of the systolic peak.

CONCLUSIONS

The results of the mathematical simulation are in agreement with the hemodynamic theory of the genesis of cerebral aneurysms. The suggested method and software complex for the multiscale simulation of CVS hemodynamics, which utilize high-performance computations, can be used at the preoperative stage for the individual evaluation of the state of the hemodynamics in the region of the cerebral aneurysm in a patient. A physician could make a decision on the choice of the strategy and tactics for the treatment of cerebral aneurysms relying on the analysis of the obtained results.

AKNOWLEDGMENTS

The study was supported by The Russian Scientific Foundation, project no. 16-15-10327

REFERENCES

1. S. E. Kornelik, E. K. Borzenko, A. N. Grishin, M. A. Bubenchikov, and V. I. Stolyarov, "Formation and destruction of erythrocyte rouleau in a vessel with local bulge," Math. Models Comput. Simul. **1**, 1–10 (2009).
2. H. J. Steiger, D. W. Liepsch, A. Poll, and H. J. Reulen, "Hemodynamic stress in terminal saccular aneurysms: a laser-Doppler study," Heart Vessels, No. **4**, 162–169 (1988).
3. F. Dorn, F. Niedermeyer, A. Balasso, D. Liepsch, and T. Liebig, "The effect of stents on intra-aneurysmal hemodynamics: in vitro evaluation of a pulsatile aneurysm using laser Doppler anemometry," Neuroradiology, No. **4**, 267–272 (2011).
4. V. A. Lishchuk, *Mathematical Theory of Blood Circulation* (Meditsina, Moscow, 1991) [in Russian].
5. S. V. Frolov, S. V. Sindeev, V. A. Lischouk, and D. Sh. Gazizova, "Hemodynamics modeling of the cardiovascular system with a pulsating heart," Trans. TSTU **13**, 546–551 (2012).
6. E. V. Astrakhantseva, V. Yu. Gidaspov, D. L. Reviznikov, "Mathematical modelling of hemodynamics of large blood vessels," Mat. Model. **17** (8), 61–81 (2005).
7. A. Ya. Bunicheva, M. A. Menyailova, S. I. Mukhin, N. V. Sosnin, and A. P. Favorskii, "Studying the influence of gravitational overloads on the parameters of blood flow in vessels of greater circulation," Math. Models Comput. Simul. **5**, 81–91 (2013).
8. N. V. Abakumov, I. V. Ashmetkov, N. B. Esikova, V. B. Koshelev, S. I. Mukhin, N. V. Sosnin, V. F. Tishkin, A. P. Favorskii, and A. B. Khrulenko, "Strategy of mathematical cardiovascular system modeling," Mat. Model. **12** (2), 106–117 (2000).
9. V. A. Lukshin, "Mathematical modeling of cerebral hemodynamics," Cand. Sci. (Phys. Math.) Dissertation (Lomonosov Moscow State Univ., Moscow, 2004).
10. V. B. Koshelev, S. I. Mukhin, T. V. Sokolova, N. V. Sosnin, and A. P. Favorskii, "Mathematical modeling of cardio-vascular hemodynamics with account of neuroregulation," Mat. Model. **19** (3), 15–28 (2007).
11. S. I. Mukhin, "Mathematical modeling of hemodynamics," Doctoral (Phys. Math.) Dissertation (Lomonosov Moscow State Univ., Moscow, 2008).
12. D. V. Ivanov and O. A. Fomkina, "Determination of constants for Neo-Hooke and Mooney–Rivlin models according to results of one-axis tension experiments," in *Collection of Scientific Articles in Mechanics and Mathematics* (Sarat. Univ., Saratov, 2008), pp. 114–117 [in Russian].
13. D. V. Ivanov and O. A. Fomkina, "Determination of mechanical properties of Willis circle arteries," Russ. J. Biomech. **12** (4), 71–78 (2008).
14. D. V. Ivanov, "Study of Willis circle arteries in normal state and with pathology," Izv. Saratov. Univ., Nov. Ser. Mat. Mekh. Inform. **10** (1), 35–43 (2010).

15. D. V. Ivanov, "Theoretical and experimental study of mechanical factors influence on the aneurysm occurence and pathogenesis in Willis circle arteries," Extended Abstract of Cand. Sci. (Phys. Math.) Dissertation (Chernyshevskii Sarat. State Univ., Saratov, 2010).

16. O. E. Pavlova, D. V. Ivanov, A. A. Gramakova, K. M. Morozov, and I. I. Suslov, "Hemodynamics and mechanical behavior of the carotid bifurcation with pathological addiction," Izv. Saratov. Univ., Nov. Ser. Mat. Mekh. Inform. **10** (2), 66–75 (2010).

17. D. V. Ivanov, A. V. Dol', O. E. Pavlova, and A. V. Aristambekova, "Modelling of human circle of Willis in normal state and with pathology," Russ. J. Biomech. **17** (3), 40–52 (2013).

18. A. Valencia, A. Contente, M. Ignat, J. Mura, E. Bravo, R. Rivera, and J. Sordo, "Mechanical test of human cerebral aneurysm sample obtained from surgical clipping," J. Mech. Med. Biol., No. 3, 28–42 (2010).

19. K. Balakhovsky, M. Jabareen, and K. Y. Volokh, "Modeling rupture of growing aneurysms," J. Biomech. **47**, 653–658 (2014).

20. C. J. Boyle, A. B. Lennon, and P. J. Prendergast, "Application of a mechanobiological simulation technique to stents used clinically," J. Biomech. **46**, 918–924 (2013).

21. A. J. Geers, I. Lararbide, H. G. Morales, and A. F. Frangi, "Approximating hemodynamics of cerebral aneurysms with steady flow simulations," J. Biomech. **47**, 178–185 (2014).

22. Y. Long, H. Yu, Z. Zhuo, Y. Zhang, Y. Wang, X. Yang, and H. Li, "A geometric scaling model for assessing the impact of aneurysm size ratio on hemodynamic characteristics," Biomed. Eng. Online, No. **17**, 13–17 (2014).

23. M. L. Baharaglu, C. M. Schirmer, D. A. Hoit, B. L. Gao, and A. M. Malek, "Aneurysm inflow-angle as a discriminant for rupture in sidewall cerebral aneurysms: morphometric and computational fluid dynamic analysis," Stroke **41**, 1423–1430 (2010).

24. J. Xiang, S. K. Natarajan, M. Tremmel, D. Ma, J. Mocco, L. N. Hopkins, A. H. Siddiqui, E. L. Levy, and H. Meng, "Hemodynamic-morphological discriminants for intracranial aneurysm, " Stroke **42**, 144–152 (2011).

25. A. M. Gambaruto, J. Janela, A. Moura, and A. Sequeira, "Sensitivity of hemodynamics in a patient specific cerebral aneurysm to vascular geometry and blood rheology," Math. Biosci. Eng. **8**, 409–423 (2011).

26. P. I. Begun, *Biomechanical Modeling of Objects Prosthetics,* The School-Book (Politekhnika, St. Petersburg, 2011) [in Russian].

27. S. Tateshima, A. Chien, J. Sayre, J. Cebral, and F. Vinuela, "The effect of aneurysm geometry on the intraaneurysmal flow condition," Neuroradiology **52**, 1135–1141 (2010).

28. S. Schnell, S. A. Ansari, P. Vakil, M. Wasielewski, M. L. Carr, M. C. Hurley, B. R. Bendok, H. Batjer, T. J. Caroll, J. Carr, and M. Markl, "Three-dimensional hemodynamics in intracranial aneurysms: influence of size and morphology," J. Magn. Reson. Imaging **39**, 120–131 (2014).

29. X. Wang and X. Li, "Biomechanical behavior of cerebral aneurysm and its relation with the formation of intraluminal thrombus: a patient-specific modelling study," Comput. Methods Biomech. Biomed. Eng. **16**, 1127–1134 (2013).

30. V. B. Parashin and G. P. Itkin, *Biomechanics of Blood Circulation,* The School-Bool, Ed. by S. I. Shchukin (Mosk. Gos. Tekh. Univ. im. N. E. Baumana, Moscow, 2005) [in Russian].

31. P. N. Watton, A. Selimovic, N. B. Raberger, P. Huang, G. A. Holzapfel, and Y. Ventikos, "Modelling evolution and the evolving mechanical environment of saccular cerebral aneurysms," Biomech. Model. Mechanobiol. **10**, 109–132 (2011).

32. M. Steinhauser, *Computational Multiscale Modeling of Fluids and Solids* (Springer, Berlin, Heidelberg, 2008).

33. V. A. Lishchuk and E. V. Mostkova, "The system of laws of the heart," Klin. Fiziol. Krovoobrashchen., No. 1, 16–21 (2006).

34. V. A. Lishchuk, S. V. Frolov, D. Sh. Gazizova, L. V. Sazykina, and S. N. Makoveev, "Mathematical model of the vessel in ordinary derivatives as a tool for vascular pathology study. Part 2," Klin. Fiziol. Krovoobrashchen., No. 1, 64–70 (2007).

Translated by A. Bigildeev